Supplementary Information

Phosphorylation amplified asymmetry of spiro[acridine-9,9'-xanthene] hosts for efficient blue and white thermal activated delay fluorescent diodes

Anqi Zhu,[1] Ying Li,[1] Yi Man,[1] Yudong Pang,[2] Chunbo Duan,[1] Chunmiao Han,[1] Jing Zhang,[1] Chenhui Cao,[2] Ying Wei,[1] Xinfeng Shui[2] and Hui Xu[1]**

[1]Key Laboratory of Functional Inorganic Material Chemistry, Ministry of Education, School of Chemistry and Material Science, Heilongjiang University, Harbin 150080, China.

[2]Anhui Sholon New Material Technology Co., Ltd., 006 Chaoyang Road, Chuzhou 239500, P. R. China.

Corresponding Authors: ywei@hlju.edu.cn (YW); hxu@hlju.edu.cn (HX).

Content

I. Experimental Section

1. Materials and Instruments

^{1}H NMR spectra were recorded using a Varian Mercury plus 400NB spectrometer relative to tetramethylsilane (TMS) as internal standard. Molecular masses were determined by a MALDI-TOF-MS. Elemental analyses were performed on a Vario EL III elemental analyzer. The crystal suitable for single-crystal XRD analysis was obtained through slowly diffusing hexane into dichloromethane solution of 27PSXADPO at room temperature. The single crystal growth of 2PSXASPO was failed, mainly because of the asymmetric molecular structure and the disordered long-range alignment. All diffraction data were collected at 295 K on a Rigaku Xcalibur E diffractometer with graphite monochromatized Mo Kα (λ = 0.71073 Å) radiation in ω scan mode. All structures were solved by direct method and difference Fourier syntheses. Non-hydrogen atoms were refined by full-matrix least-squares techniques on F2 with anisotropic thermal parameters. The hydrogen atoms attached to carbons were placed in calculated positions with C−H = 0.93 Å and U(H) = 1.2Ueq(C) in the riding model approximation. All calculations were carried out with the SHELXL97 program. Absorption and photoluminescence (PL) emission spectra of the target compound were measured using a SHIMADZU UV-3150 spectrophotometer and a SHIMADZU RF-5301PC spectrophotometer, respectively. Thermogravimetric analysis (TGA) and differential scanning calorimetry (DSC) were performed on Shimadzu DSC-60A and DTG-60A thermal analyzers under nitrogen atmosphere at a heating rate of 10 °C min^{-1}. Cyclic voltammetric (CV) studies were conducted using an Eco Chemie B. V. AUTOLAB potentiostat in a typical three-electrode cell with a glassy carbon working electrode, a platinum wire counter electrode, and a silver/silver chloride (Ag/AgCl) reference electrode. All electrochemical experiments were carried out under a nitrogen atmosphere at room temperature in dichloromethane. Phosphorescence spectra were measured in dichloromethane using an Edinburgh FPLS 1000 fluorescence spectrophotometer at 77 K cooling by liquid nitrogen with a

delay of 300 μs using Time-Correlated Single Photon Counting (TCSPC) method with a microsecond pulsed Xenon light source for 10 μs-10 s lifetime measurement, the synchronization photomultiplier for signal collection and the Multi-Channel Scaling Mode of the PCS900 fast counter PC plug-in card for data processing. The TADF dye doped films (100 nm) were prepared through vacuum evaporation for optical analysis. Photoluminescence quantum yields (PLQY, ϕ_{PL}) of these films were measured through a labsphere 1-M-2 (ϕ = 6") integrating sphere coated by Benflect with efficient light reflection in a wide range of 200-1600 nm, which was integrated with FPLS 1000. The absolute η_{PL} determination of the sample was performed by two spectral (emission) scans, with the emission monochromator scanning over the Rayleigh scattered light from the sample and from a blank substrate. The first spectrum recorded the scattered light and the emission of the sample, and the second spectrum contained the scattered light of Benflect coating. The integration and subtraction of the scattered light parts in these two spectra arrived at the photon number absorbed by the samples (N_a); while, integration of the emission of the samples to calculate the emissive photon number (N_e). Then, the absolute ϕ_{PL} can be estimated according to the equation of $\eta_{PL} = N_e/N_a$. Spectral correction (emission arm) was applied to the raw data after background subtraction, and from these spectrally corrected curves the quantum yield was calculated using aF900 software wizard.

2. DFT Calculations

DFT computations were carried out with different parameters for structure optimizations and vibration analyses. The ground state configuration was optimized by the restricted and unrestricted formalism of Beck's three-parameter hybrid exchange functional[1] and Lee, and Yang and Parr correlation functional[2] B3LYP/6-31G(d,p), respectively. The fully optimized stationary points were further characterized by harmonic vibrational frequency analysis to ensure that real local minima had been found without imaginary vibrational frequency. The contours were visualized with Gaussview 5.0. All computations were performed using the Gaussian 09 package.[3]

3. Device Fabrication and Testing

Before loading into a deposition chamber, the ITO substrate was cleaned with detergents and deionized water, dried in an oven at 120 °C for 4 h, and treated with oxygen plasma for 3 min. Devices were fabricated by evaporating organic layers at a rate of 0.1-0.2 nm s^{-1} onto the ITO substrate sequentially at a pressure below 4×10^{-4} Pa. Onto the electron-transporting layer, a layer of LiF with 1 nm thickness was deposited at a rate of 0.1 nm s^{-1} to improve electron injection. Finally, a 100-nm-thick layer of Al was deposited at a rate of 0.6 nm s^{-1} as the cathode. The emission area of the devices was 0.09 cm^2 as determined by the overlap area of the anode and the cathode. After fabrication, the devices were immediately transferred to a glove box for encapsulation with glass cover slips using epoxy glue. The EL spectra and CIE coordinates were measured using a PR655 spectra colorimeter. The current density-voltage and brightness–voltage curves of the devices were measured using a Keithley 4200 source meter and a calibrated silicon photodiode. All the measurements were carried out at room temperature under ambient conditions. For each structure, four devices were fabricated in parallel to confirm the performance repeatability. To make conclusions reliable, the data reported herein were most close to the average results.

4. Synthesis

All the reagents used for synthesis were purchased from Alfa and Sinopharm Chemical Reagent Co., Ltd, and used without further purification.

*10-phenyl-10H-spiro[Acridine-9,9′ -Xanthene] (**PSXA**)*: In a nitrogen atmosphere, 50 mL of anhydrous THF solution was added to *o*-bromotrianiline (2.48 g, 10 mmol) and cooled to -78 °C. N-butyllithium solution (2.5M in hexane, 8.8mL, 22 mmol) was slowly added into the reaction solution and stirred for 1 hour. Then, Xanthone (1.98g, 11 mmol) was added and stirred at temperature for 0.5 hour. Gradually bring the reaction system back to room temperature and stir overnight. After quenching with a small amount of water, the resulting reaction solution was extracted with chloroform. The organic layer was washed with water and the aqueous phase was extracted with chloroform 3 times. The combined chloroform layer was dried with anhydrous

sodium sulfate and spun dry concentrated to obtain hydroxyl intermediates. The crude hydroxyl intermediates were diluted with chloroform (30 mL) and added with methyl sulfonic acid (32 mL, 10 mmol). After dripping, reflux was carried out for 2 h. After cooling to room temperature, the reaction mixture was cleaned with saturated K_2CO_3 solution (30 mL), and the resulting solution was extracted with water and methylene chloride. The organic phase was dried by anhydrous Na_2SO_4. The solvent is removed in a vacuum. The residue was purified by flash column chromatography and white crystal with yield of 31% was obtained. ^{1}H NMR (TMS, $CDCl_3$, 400 MHz): δ = 7.738-7.700 (t, J = 7.6 Hz, 2H); 7.606-7.569 (t, J = 7.4 Hz, 1H); 7.489-7.469 (d, J = 7.2 Hz, 2H); 7.217-7.170 (m, 6H); 6.999-6.959 (m, 2H); 6.921-6.880 (m, 4H); 6.717-6.678 (t, J = 7.6 Hz, 2H); 6.331-6.290 ppm (d, J = 8.4 Hz, 2H); LDI-TOF: m/z (%): 423.16 (100) [M^+]; elemental analysis (%) for $C_{31}H_{21}NO$: C, 87.92; H, 5.00; N, 3.31; O, 3.78.

*diphenyl(10-phenyl-10H-spiro[Acridine-9,9'-xanthen]-2-yl)phosphine oxide **(2PSXASPO)***: Step one: Under the condition of ice water bath, 20 mL ice acetic acid was added into a flask containing **PSXA** (4.23 g, 10 mmol) and kept for 15 min. Half NBS (1.7 g, 10 mmol) was added into the flask in batches and measured at intervals of half an hour until the raw material disappeared. The mixture was extracted with DCM. The organic layer was collected and extracted with saturated sodium bicarbonate aqueous solution. The organic phase was dried with anhydrous Na_2SO_4. Then, the solvent was removed by vacuum method, and the residue was purified by flash column chromatography. The yield of **2PSXASBr** was 50%. ^{1}H NMR (TMS, $CDCl_3$, 400 MHz): δ = 7.712-7.674 (t, J = 7.6 Hz, 2H); 7.587-7.550 (t, J = 7.2 Hz, 1H); 7.430-7.409 (d, J = 8.4 Hz, 2H); 7.217-7.128 (m, 6H); 6.991-6.920 (m, 4H); 6.891-6.809 (m, 2H); 6.695-6.656 (t, J = 7.6 Hz, 1H); 6.265-6.246 (d, J = 7.6 Hz, 1H); 6.169-6.147 ppm (d, J = 8.8 Hz, 1H); LDI-TOF: m/z (%):501.07 (100) [M^+]; elemental analysis (%) for $C_{31}H_{20}BrNO$: C, 74.11; H, 4.01; Br, 15.90; N, 2.79; O, 3.18.

Step two: Under a nitrogen atmosphere, n-butyl lithium (2.5 M in hexane, 4.4 mL, 11 mmol) was added to **2PSXASBr** (5.02 g, 10 mmol) anhydrous THF (20 mL)

solution under nitrogen atmosphere at -78 °C. After stirring for 1 hour, Ph_2PCl (0.75 mL, 11 mmol) was slowly added while the solution was stirred at temperature and the reaction was stirred overnight. After a small amount of water was quenched, chloroform was used to dissolve and extract the organic layer. Then hydrogen peroxide was added at 0 °C and stirred for 4 h. After quenching with a small amount of water, the reactants were concentrated and extracted by chloroform, the solvent was removed by vacuum, and the residues were purified by flash column chromatography. White crystals with a yield of 16% were obtained. ^{1}H NMR (TMS, $CDCl_3$, 400 MHz): δ = 7.729-7.691 (t, J = 7.6 Hz, 2H); 7.608-7.571 (t, J = 7.4 Hz; 1H); 7.455-7.419 (m, 4H); 7.395-7.344 (m, 4H); 7.304-7.259 (m, 3H); 7.239-7.206 (m, 1H); 7.189-7.140 (m, 2H); 7.105-7.082 (dd, J_1 = 1.2 Hz, J_2 = 1.6 Hz, 2H); 7.055-7.033 (dd, J_1 = 0.8 Hz, J_2 = 0.8 Hz, 2H); 7.013-6.892 (m, 5H); 6.772-6.732 (m, 1H); 6.356-6.317 ppm (m, 2H); LDI-TOF: m/z (%):623.20 (100) [M^+]; elemental analysis (%) for $C_{43}H_{30}NO_2P$: C, 82.81; H, 4.85; N, 2.25; O, 5.13; P, 4.97.

(10-phenyl-10H-spiro[acridine-9,9'-Xanthene]-2,7-diyl)bis(diphenylphosphine oxide) ***(27PSXADPO)***: (10-Phenyl - 10h-spiro [Acridine -9,9'-xanthene]-2,7-diyl) : Step one: Under the condition of ice water bath, 40 mL ice acetic acid was added into a flask containing **PSXA** (4.23 g, 10 mmol) and kept for 15 min. Half NBS (3.5 g, 20 mmol) was added into the flask in batches and measured at intervals of half an hour until the raw material disappeared. The mixture was extracted with DCM. The organic layer was collected and extracted with saturated sodium bicarbonate aqueous solution. The organic phase was dried with anhydrous Na_2SO_4. Then, the solvent was removed by vacuum method and the residue was purified by flash column chromatography. The yield of **27PSXADBr** was 45%. ^{1}H NMR (TMS, $CDCl_3$, 400 MHz): δ = 7.740-7.702 (t, J = 8.0 Hz, 2H); 7.622-7.585 (t, J = 7.6 Hz, 1H); 7.423-7.405 (d, J = 7.2 Hz, 2H); 7.276-7.198 (m, 5H); 7.133-7.110 (dd, J_1 = 8.0 Hz, J_2 = 1.6 Hz, 2H); 7.037-6.964 (m, 4H); 6.912-6.906 (d, J = 2.4 Hz, 2H); 6.178-6.156 ppm (d, J = 8.8 Hz, H); LDI-TOF: m/z (%):580.98 (100) [M^+]; elemental analysis (%) for $C_{31}H_{19}Br_2NO$: C, 64.05; H, 3.29; Br, 27.49; N, 2.41; O, 2.75. CCDC number: 2287105.

Step two: Under a nitrogen atmosphere, n-butyl lithium (2.5 M in hexane, 8.8 mL, 22 mmol) was added to the anhydrous THF (40 mL) solution of **27PSXADBr** (5.81 g, 10 mmol) under nitrogen atmosphere at -78 °C. After stirring for 1 hour, Ph_2PCl (1.5 mL, 22 mmol) was slowly added, while the solution was stirred at temperature and the reaction was stirred overnight. After a small amount of water was quenched, chloroform was used to dissolve and extract the organic layer. Then hydrogen peroxide was added at 0 °C and stirred for 4 h. After quenching with a small amount of water, the reactants were concentrated and extracted by chloroform, the solvent was removed by vacuum, and the residues were purified by flash column chromatography. White crystals with a yield of 23% were obtained. ^{1}H NMR (TMS, $CDCl_3$, 400 MHz): δ = 7.724-7.686 (t, *J* = 7.6 Hz, 2H); 7.617-7.579 (m, 1H); 7.487-7.451 (t, *J* = 7.2 Hz, 4H); 7.418-7.345 (m, 10H); 7.321-7.297 (m, 8H); 7.258-7.227 (d, *J* = 12.4 Hz, 2H); 7.152-7.116 (t, *J* = 7.2 Hz, 2H); 7.035-6.908 (m, 8H); 6.413-6.387ppm (dd, J_1 = 1.6 Hz, J_2 = 1.6 Hz, 2H); LDI-TOF: m/z (%):823.24 (100) [M^+]; elemental analysis (%) for $C_{55}H_{39}NO_3P_2$: C, 80.18; H, 4.77; N, 1.70; O, 5.83; P, 7.52.

II. Single Crystal Packing

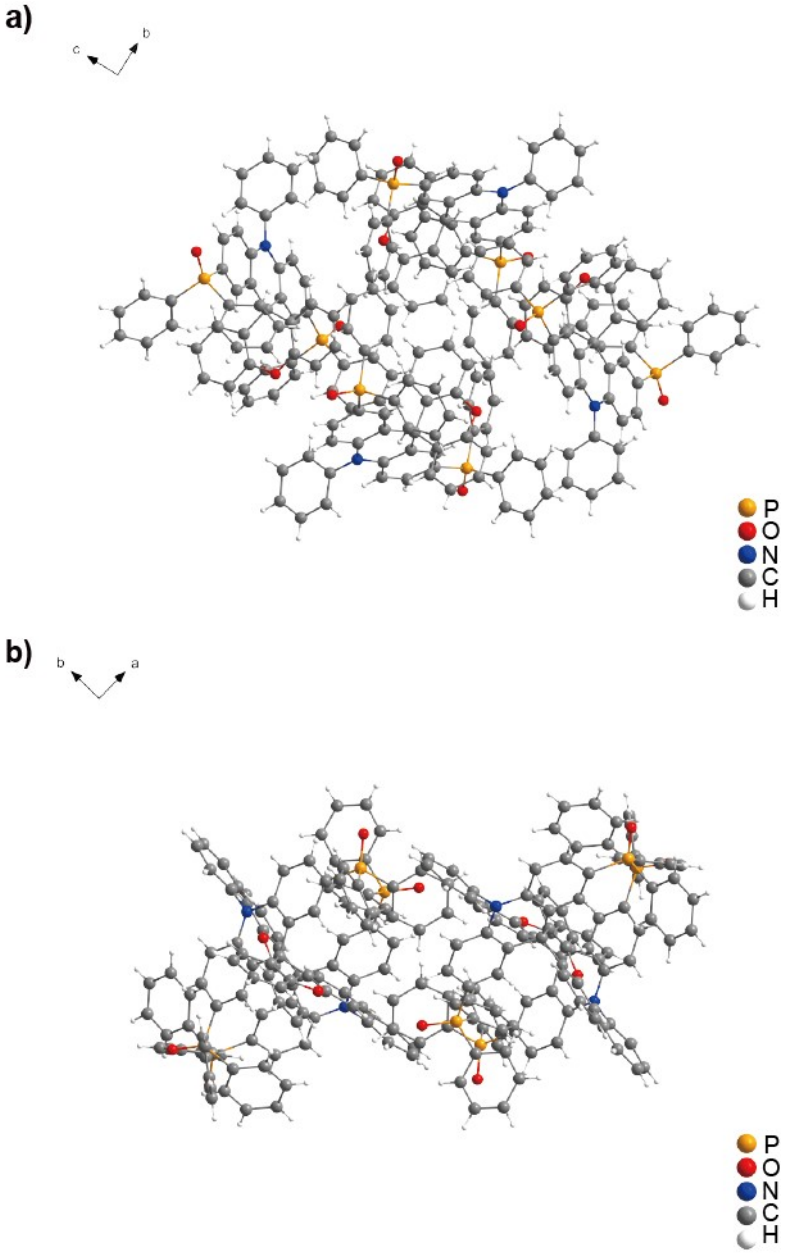

Figure S1. Single-crystal structure of 27PSXADPO; a) packing diagram along *a* axis; b) packing diagram along *c* axis;

III. Thermal Properties

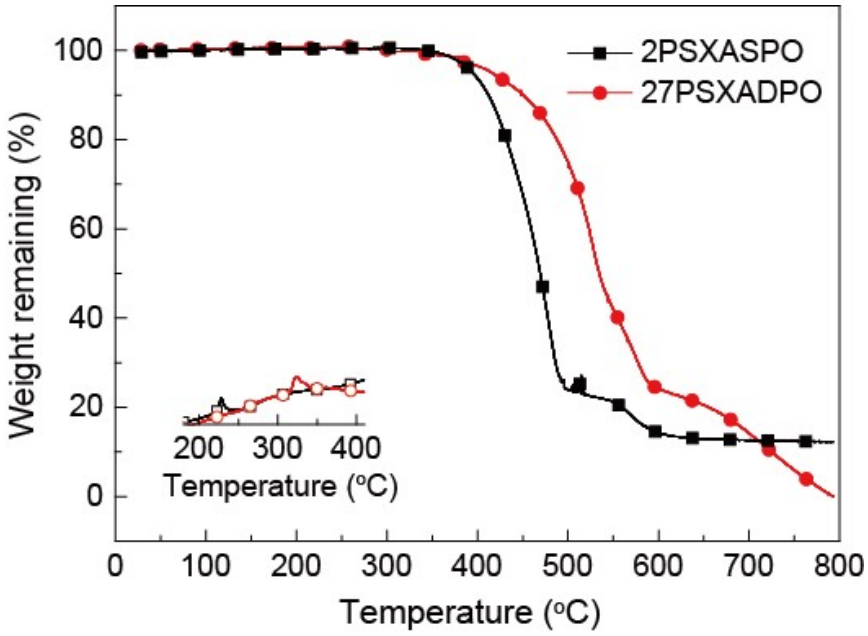

Figure S2. TGA and DSC (inset) curves of **2PSXASPO** and **27PSXADPO**.

IV. Compatibility with TADF Dopants

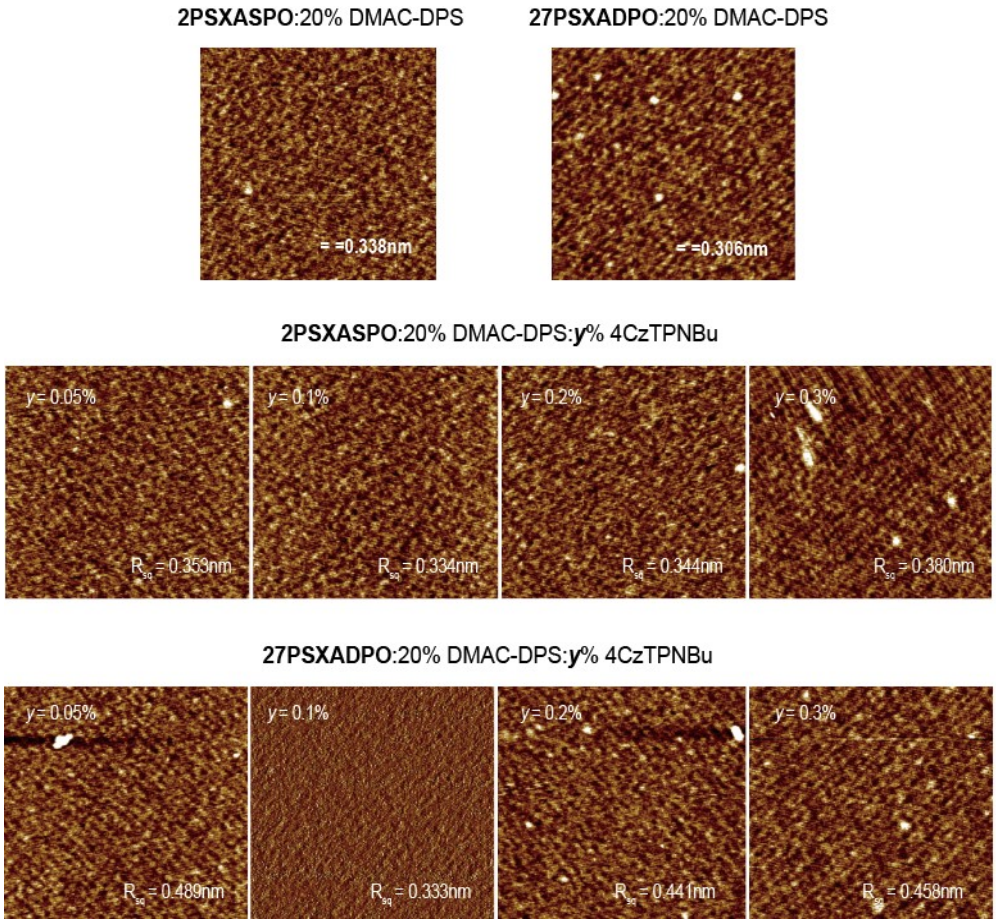

Figure S3. AFM images of the *vacuum*-evaporated **2PSXASPO** and **27PSXADPO** (100 nm) with different doping concentrations of DMAC-DPS and 4CzTPN-Bu. Scanning area: 3 × 3 μm.

V. Gaussian simulation result

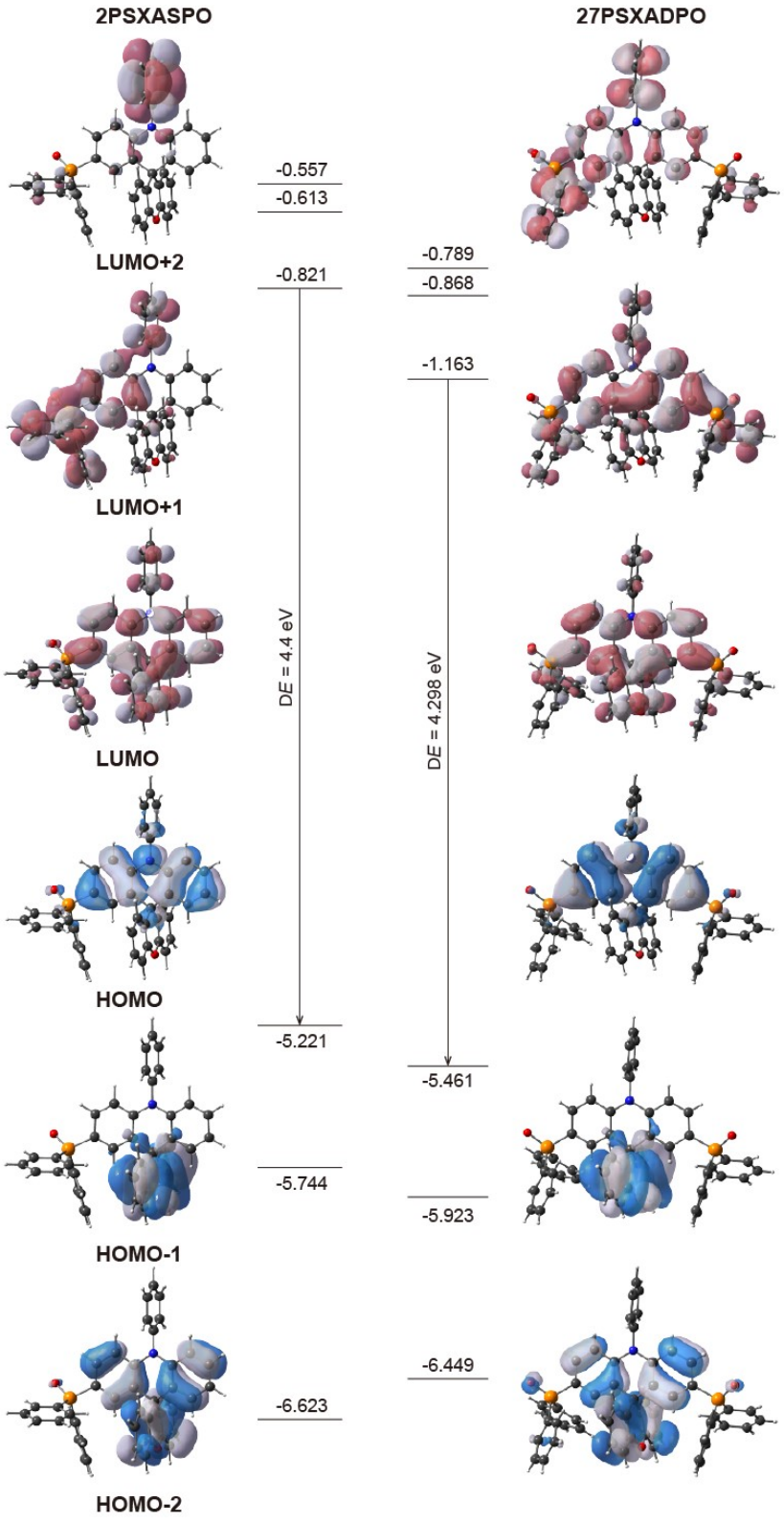

Figure S4. Contours and energy levels of frontier molecular orbitals for **2PSXASPO** and **27PSXADPO**.

VI. Electrochemical property

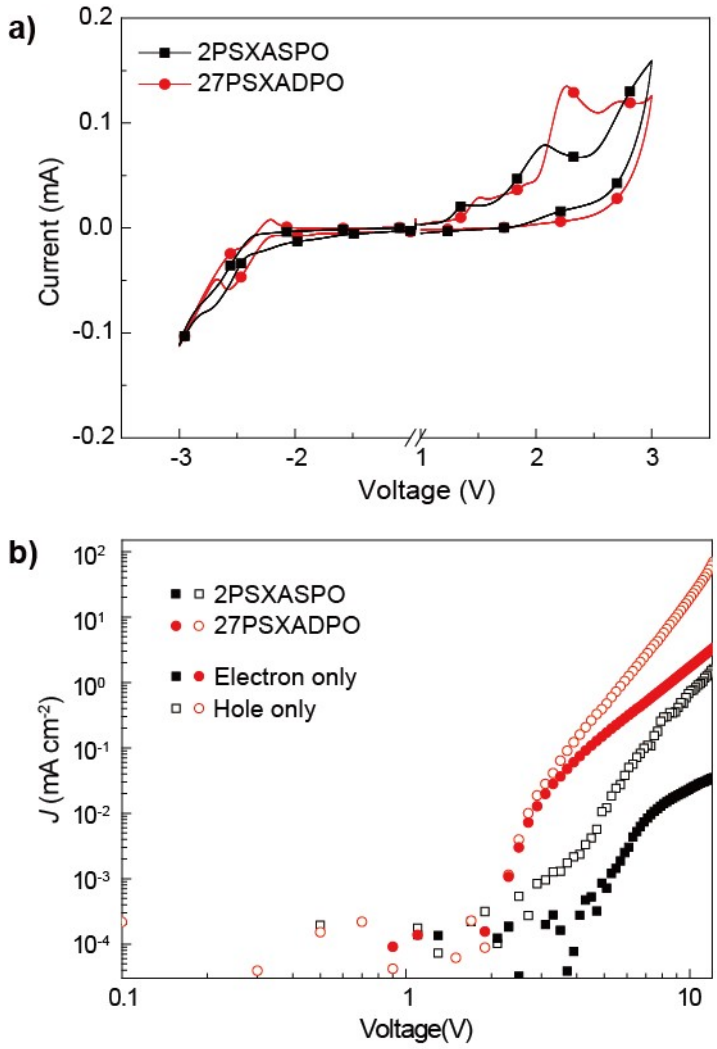

Figure S5. a) CV curves of **2PSXASPO** and **27PSXADPO** measured at room temperature with the scanning rate of 100 mV s^{-1}; b) *I-V* characteristics of nominal singlecarrier-only devices based on **2PSXASPO** and **27PSXADPO** with the structures of ITO|MoO_3 (5 nm)|PO (100 nm)|MoO_3 (5 nm)|Al for hole-only and ITO|LiF (1 nm)|PO (100 nm)|LiF (1 nm)|Al for electron-only.

VII. Photophysical property

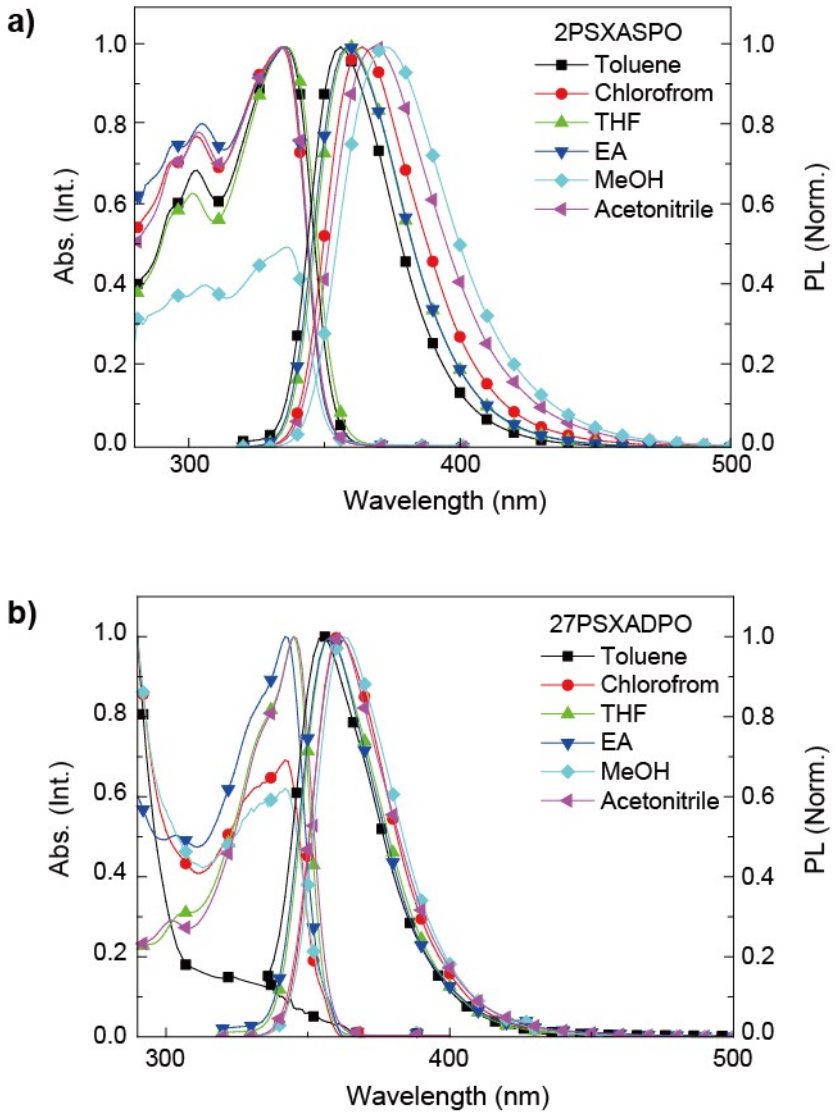

Figure S6. PL spectra of **2PSXASPO** a) and **27PSXADPO** b) in solvents with different polarities (10^{-6} mol L^{-1}).

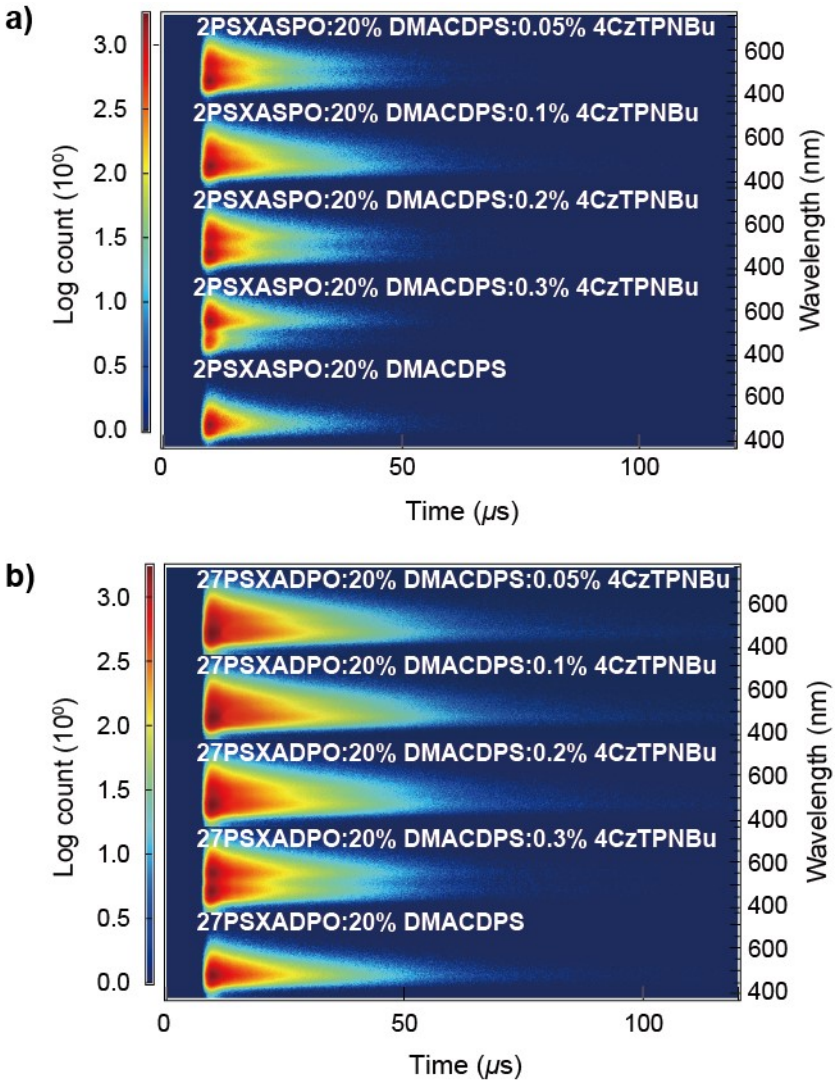

Figure S7. Time-resolved emission contours of *vacuum*-evaporated **2PSXASPO** and **27PSXADPO** films doped with 20% DMAC-DPS: *y*% 4CzTPNBu (*y* = 0.05, 0.1, 0.2 and 0.3 100 nm).

Table S1. Photophysical properties of **2PSXASPO** and **27PSXADPO**.

Compound	Absorption (nm)	Emission (nm)	FWHM (nm)	S_1 (eV)	T_1 (eV)	T_m/T_d (°C)	HOMO (eV)	LUMO (eV)
2PSXASPO	345, 307, 248, 229[a]	364[a]	38[a]	3.64[c]	2.77[e]	228/394	-5.96[f]	-2.48[f]
	339, 281[b]	401[b]	72[b]	3.78[d]	3.08[d]		-5.22[d]	-0.82 [d]
27PSXADPO	338, 305, 246, 230[a]	361[a]	30[a]	3.62[c]	2.77[e]	324/415	-6.07 [f]	-2.58[f]
	346, 283[b]	374[b]	41[b]	3.70[d]	2.92[d]		-5.46[d]	-1.16[d]

[a]In CH_2Cl_2 (10^{-6} mol L^{-1}); [b]in film; [c]estimated according to the fluorescence spectra; [d]Gaussian simulation results; [e]calculated according to 0-0 transition of PH emission; [f]estimated according to the equation HOMO/LUMO = 4.78 + onset voltage.

VIII. Electroluminescence property

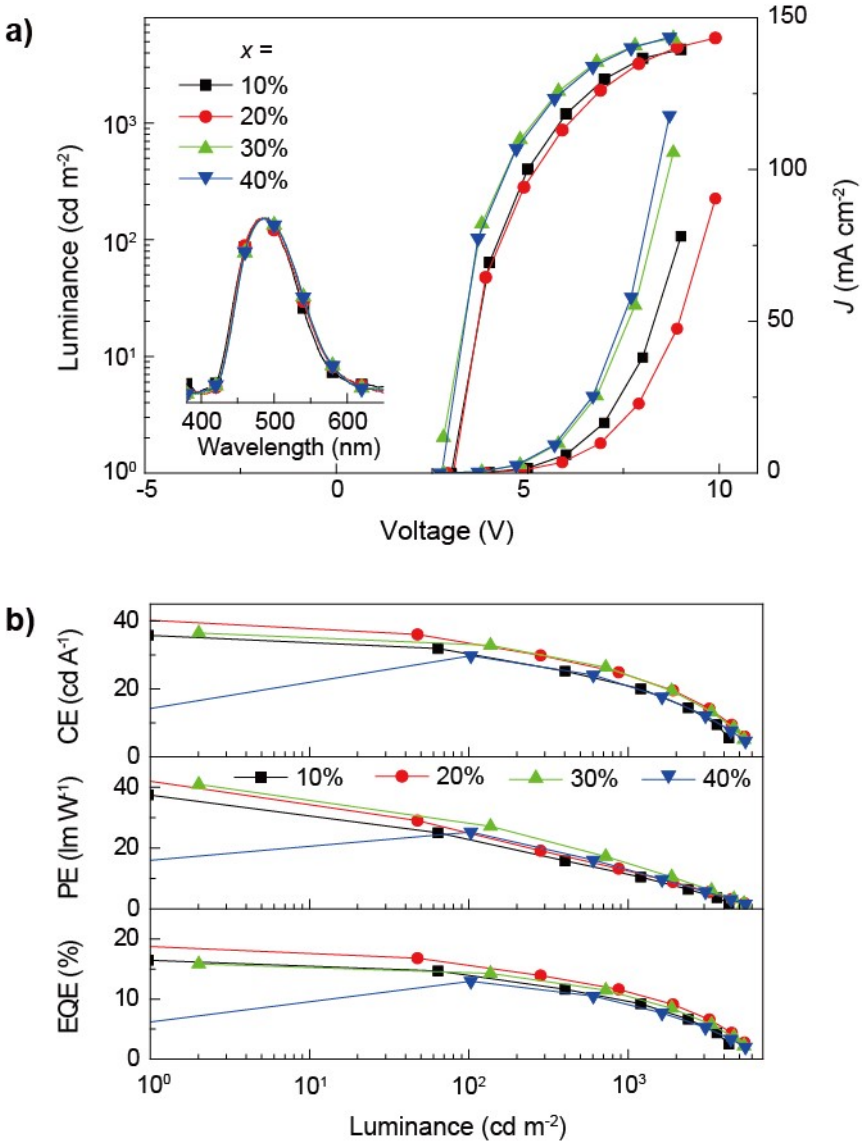

Figure S8. Device performance of blue TADF diodes based on **27PSXADPO** with emissive layers of PO host:*x*% DMACDPS. a) Electroluminescent spectra (insets) at 1000 nits and luminance-voltage-current density (*J*) relationships; b) efficiency vs. Luminance relationships of the devices at *x* = 10~40;

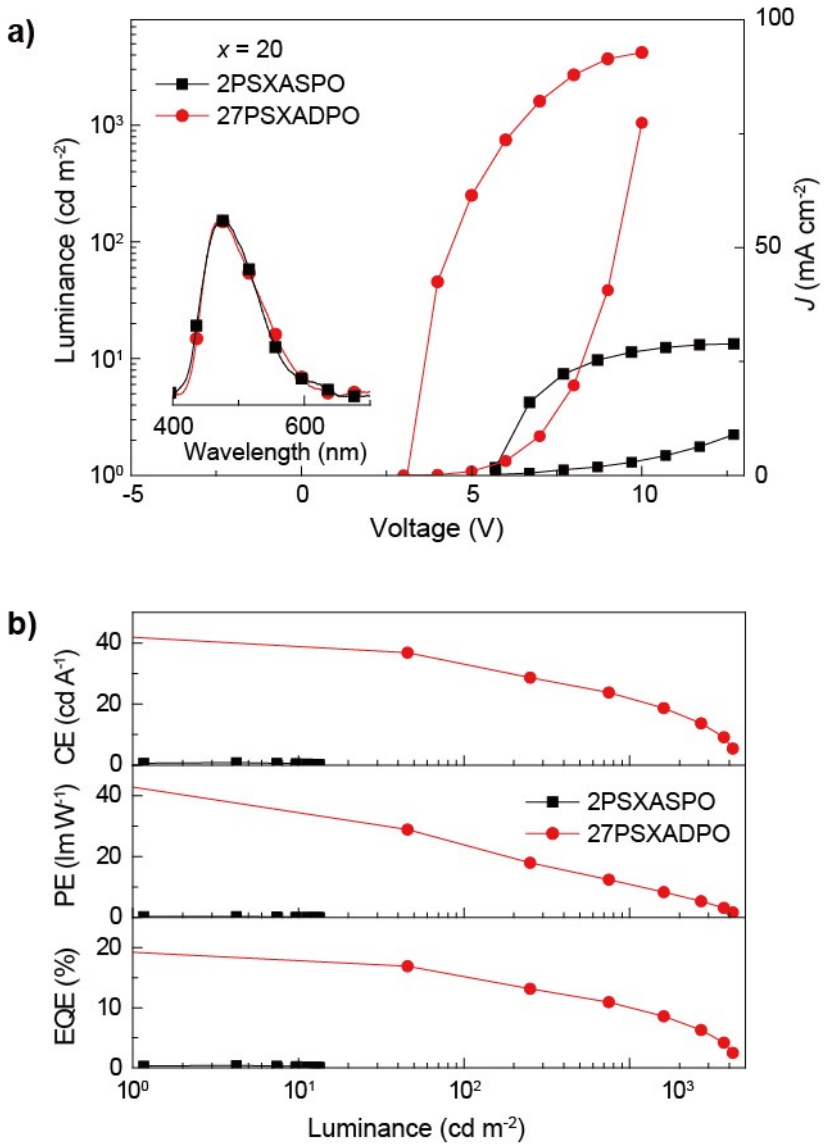

Figure S9. Device performance of blue TADF diodes based on **2PSXASPO** and **27PSXADPO** with emissive layers of PO host:20% DMACDPS. a) Electroluminescent spectra (insets) at 1000 nits and luminance-voltage-current density (*J*) relationships; b) Efficiency-luminance relationships.

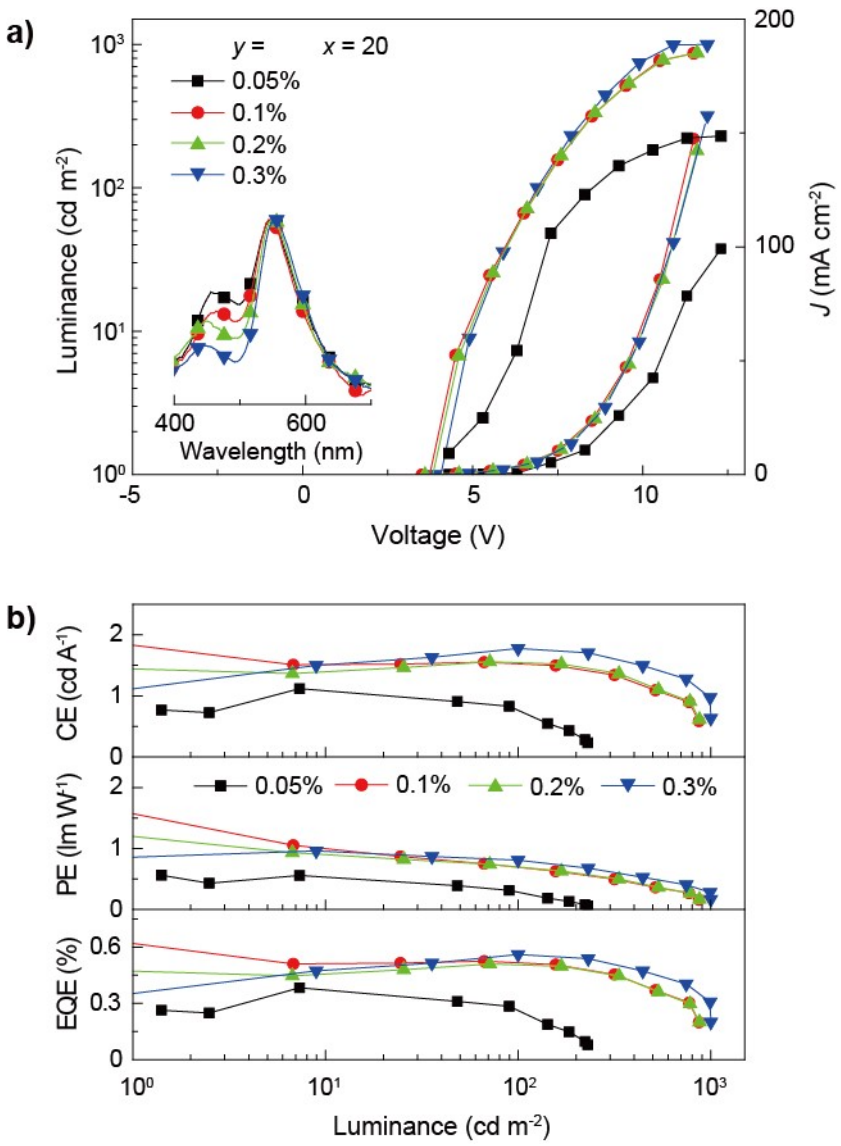

Figure S10. EL performance of **2PSXASPO**:20% DMAC-DPS:*y*% 4CzTPNBu based WOLEDs (*y* = 0.05~0.3). a) Luminance (*L*)-Voltage (*V*)-Current density (*J*) curves , and b) efficiency vs. Luminance relationships of the devices.

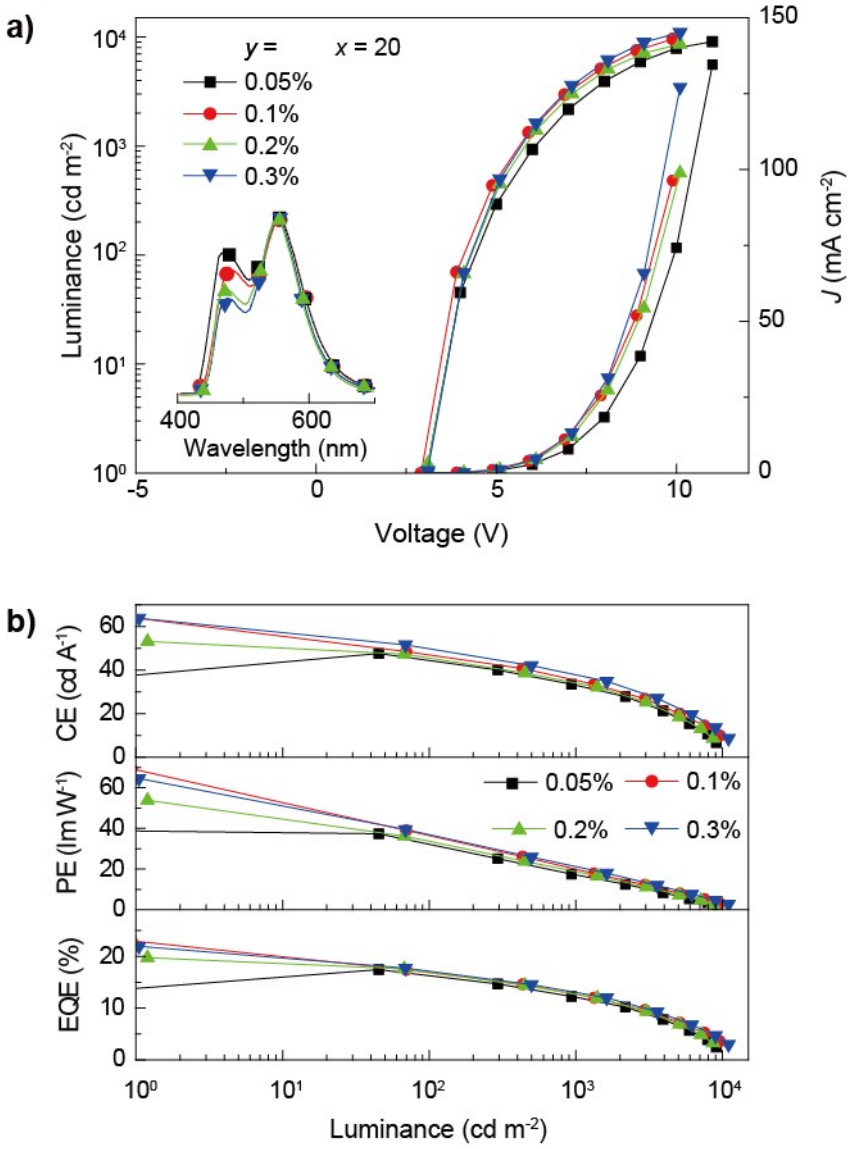

Figure S11. EL performance of **27PSXADPO**:20% DMAC-DPS:*y*% 4CzTPNBu based WOLEDs (y = 0.05~0.3). a) Luminance (L)-Voltage (V)-Current density (J) curves, and b) efficiency vs. Luminance relationships of the devices.

Table S2. EL performance of WOLEDs based on **2PSXASPO** and **27PSXADPO**.

EML	V_{on}[a] (V)	L_{max}[b] (cd m^{-2})	η_{CE}[c] (cd A^{-1})	η_{PE}[c] (lm W^{-1})	η_{EQE}[c] (%)	CIE/λ_{EL}[d]
	-		-	-	-	
2PSXASPO: 20 wt % DMACDPS: 0.05 wt % 4CzTPNBu	8.5	230	0.7	0.2	0.2	0.3423, 0.4598/465, 546
	-		-	-	-	
	3.5		1.9	1.7	0.6	
2PSXASPO: 20 wt % DMACDPS: 0.1 wt % 4CzTPNBu	7.0	1717	1.5	0.7	0.5	0.3643, 0.4773/464, 547
	-		-	-	-	
	3.9		1.4	1.2	0.4	
2PSXASPO: 20 wt % DMACDPS: 0.2 wt % 4CzTPNBu	6.9	874	1.5	0.6	0.5	0.3919, 0.4936/448, 551
	-		-	-	-	
	4.1		1.1	0.8	0.3	
2PSXASPO: 20 wt % DMACDPS: 0.3 wt % 4CzTPNBu	7.0	1000	1.7	0.8	0.5	0.4146, 0.5100/445, 554
	11		0.6	0.1	0.2	

	3.0		37.8	38.7	13.7	
27PSXADPO: 20 wt % DMACDPS: 0.05 wt % 4CzTPNBu	4.4	9138	44.3	32.1	16.2	0.2778, 0.4018/477, 549
	6.0		33	17.2	12.1	
	2.9		64.0	69.3	22.9	
27PSXADPO: 20 wt % DMACDPS: 0.1 wt % 4CzTPNBu	4.1	18310	46.8	36.5	16.8	0.3045, 0.4118/469, 548
	5.6		35.3	19.8	12.6	
	3.0		-	-	-	
27PSXADPO: 20 wt % DMACDPS: 0.2 wt % 4CzTPNBu	4.2	8622	45.5	33.7	16.9	0.3336, 0.4475/467, 554
	5.8		34.1	18.6	12.5	
	4.1		63.8	64.9	21.9	
27PSXADPO: 20 wt % DMACDPS: 0.3 wt % 4CzTPNBu	7.0	1000	49.6	37.0	17	0.3636, 0.4724/463, 554
	11		37.8	21.2	13	

[a] At 1, 100 and 1000 cd m^{-2}; [b] the maximum luminance; [c] EL efficiencies at the maximum and 100 and 1000 cd m^{-2}; [d] peak wavelengths and CIE coordinates of EL emissions at 1000 cd m^{-2}.

IX. ^{1}H NMR Spectra

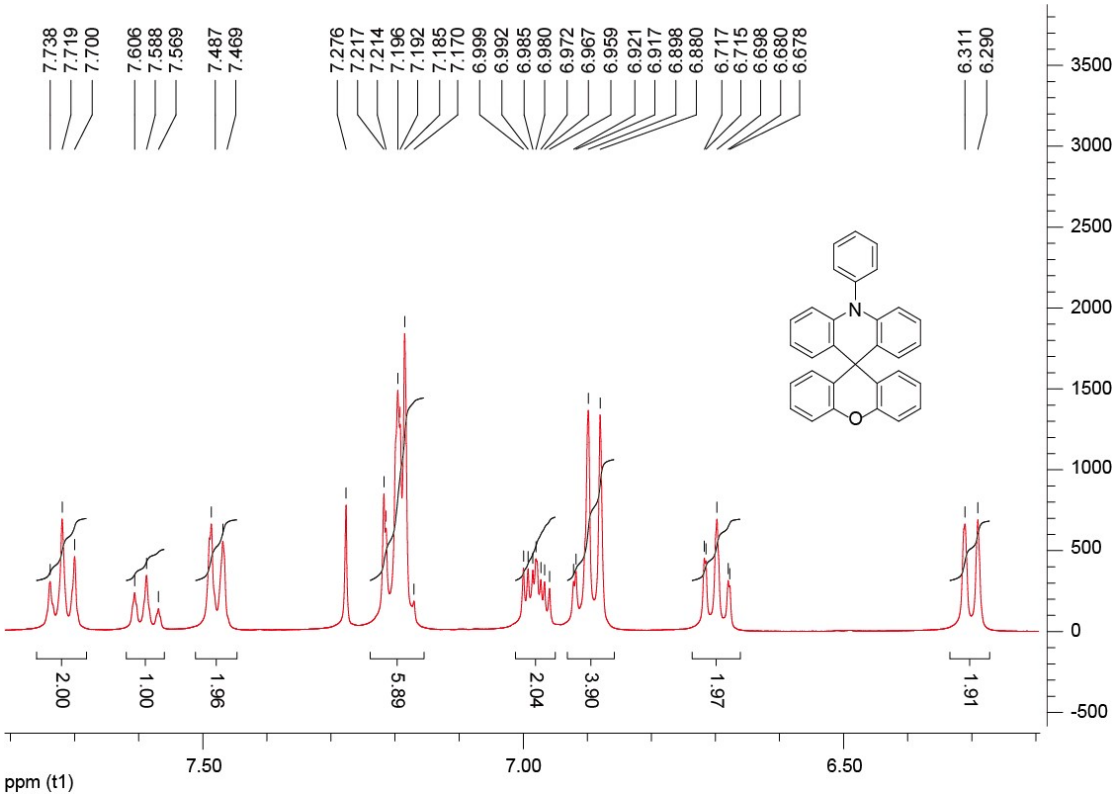

Figure S12. ^{1}H NMR spectrum of **PSXA** ($CDCl_3$, with TMS).

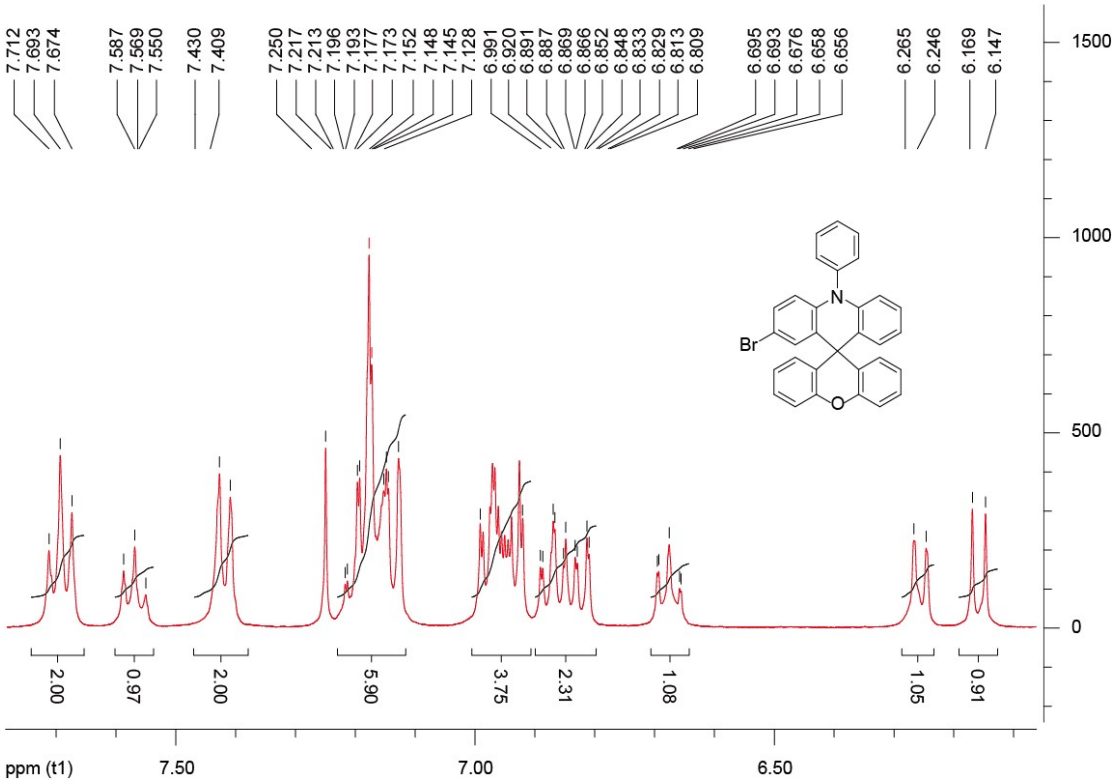

Figure S13. ^{1}H NMR spectrum of **2PSXASBr** ($CDCl_3$, with TMS).

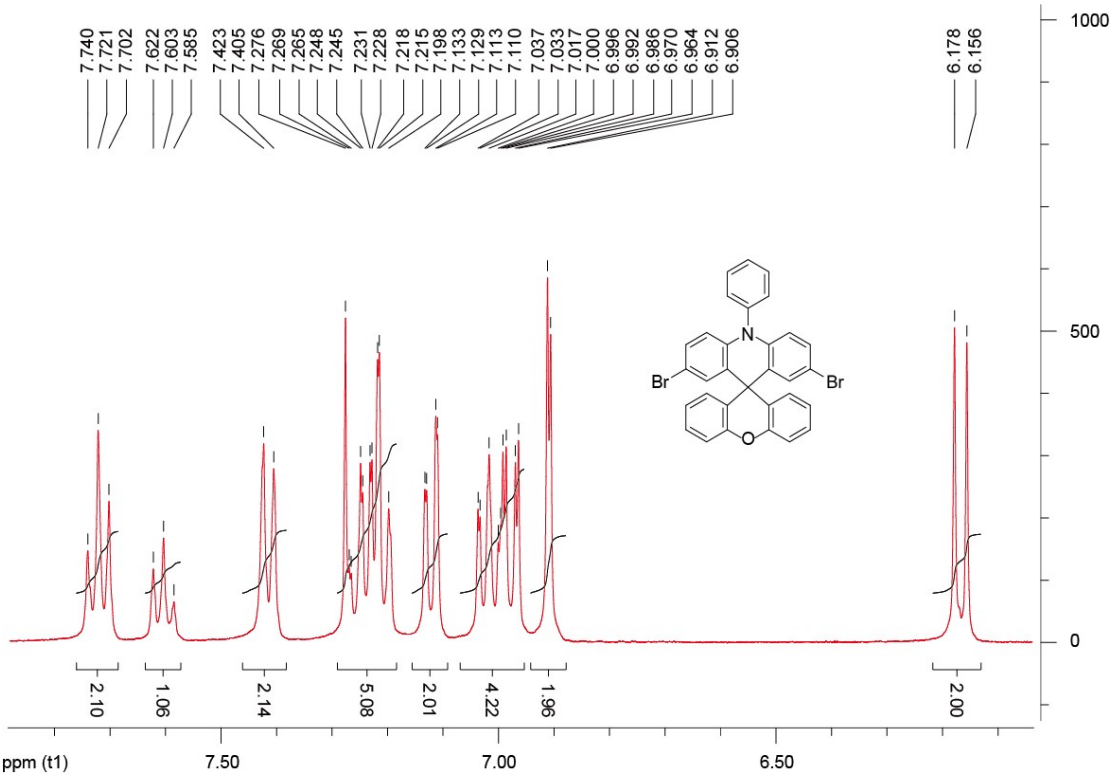

Figure S14. ^{1}H NMR spectrum of **27PSXADBr** ($CDCl_3$, with TMS).

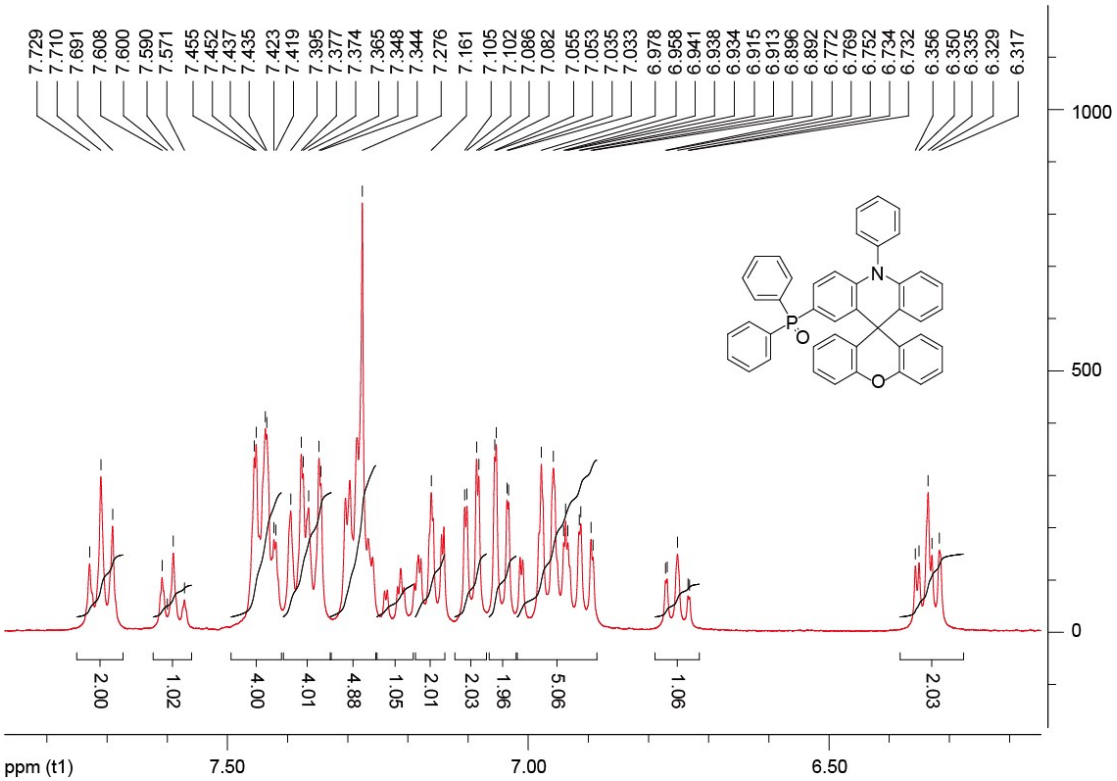

Figure S15. ^{1}H NMR spectrum of **2PSXASPO** ($CDCl_3$, with TMS).

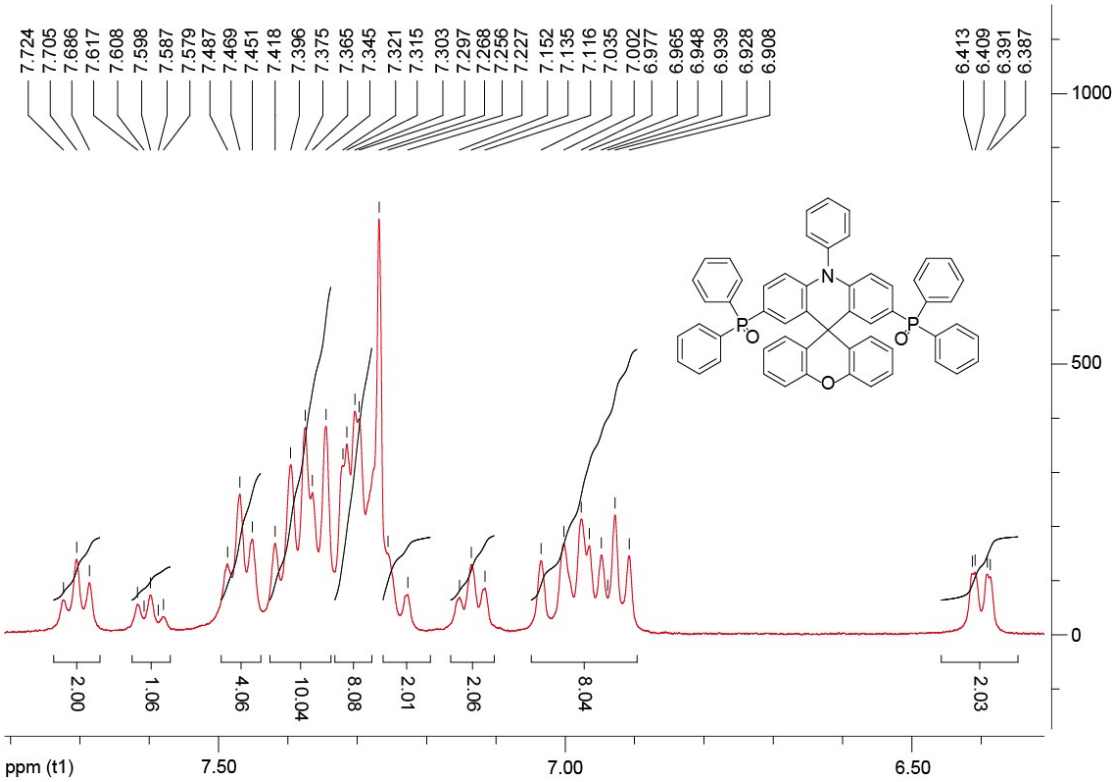

Figure S16. ^{1}H NMR spectrum of **27PSXADPO** ($CDCl_3$, with TMS).

X. References

[1] A. D. Becke, *J. Chem. Phys.* **1993**, *98*, 5648-5652.

[2] C. Lee, W. Yang, R. G. Parr, *Phys. Rev. B* **1988**, *37*, 785-789.

[3] M. J. Frisch, G. W. Trucks, H. B. Schlegel, G. E. Scuseria, M. A. Robb, J. R. Cheeseman, J. A. Montgomery, J. T. Vreyen, K. N. Kudin, J. C. Burant, J. M. Millam, S. S. Iyengar, J. Tomasi, V. Barone, B. Mennucci, M. Cossi, G. Scalmani, N. Rega, G. A. Petersson, H. Nakatsuji, M. Hada, M. Ehara, K. Toyota, R. Fukuda, J. Hasegawa, M. Ishida, T. Nakajima, Y. Honda, O. Kitao, H. Nakai, M. Klene, X. Li, J. E. Knox, H. P. Hratchian, J. B. Cross, C. Adamo, J. Jaramillo, R. Gomperts, R. E. Stratmann, O. Yazyev, A. J. Austin, R. Cammi, C. Pomelli, J. W. Octhterski, P. Y. Ayala, K. Morokuma, G. A. Voth, P. Salvador, J. J. Dannenberg, V. G. Zakrzewski, S. Dapprich, A. D. Daniels, M. C. Strain, O. Farkas, D. K. Malick, A. D. Rabuck, K. Raghavachari, J. B. Foresman, J. V. Ortiz, Q. Cui, A. G. Baboul, S. Clifford, J. Cioslowski, B. B. Stefanov, A. L. G. Liu, P. Piskorz, I. Komaromi, R. L.Martin, D. J. Fox, T. Keith, M. A. Al-Laham, C. Y. Peng, A. Nanayakkara, M. Challacombe, P. M. W. Gill, B. Johnson, W. Chen, M. W. Wong, C. Gonzalez, J. A. Pople, *Gaussian 03, Revision D.02, Gaussian Inc., Pittsburgh, PA* **2004**.